Cation Binding in Na,K-ATPase, Investigated by ^{205}Tl Solid-State NMR Spectroscopy†

Louise Odgaard Jakobsen,‡ Anders Malmendal,§ Niels Chr. Nielsen,§ and Mikael Esmann*,‡

Department of Biophysics, Institute of Physiology and Biophysics, University of Aarhus, DK-8000 Aarhus, Denmark, and Center for Insoluble Protein Structures (inSPIN), Interdisciplinary Nanoscience Center (iNANO) and Department of Chemistry, University of Aarhus, DK-8000 Aarhus, Denmark

Received April 1, 2006; Revised Manuscript Received July 7, 2006

ABSTRACT: Cation binding to Na,K-ATPase is characterized in native membranes at room temperature by solid-state NMR spectroscopy using the K^+ congener ^{205}Tl. It has been demonstrated that the signals from occluded Tl^+ and nonspecifically bound Tl^+ can be detected and distinguished by NMR. Effects of dipole−dipole coupling between ^{1}H and ^{205}Tl in the occlusion sites show that the ions are rigidly bound, rather than just occluded. Furthermore, a low chemical shift suggests occlusion site geometries with a relatively small contribution from carboxylate and hydroxyl groups. Nonspecific binding of Tl^+ is characterized by rapid chemical exchange, in agreement with the observed low binding affinity.

Na,K-ATPase is a membrane-bound enzyme responsible for the active transport of three Na^+ ions out of and two K^+ ions into the cell, in both cases against their chemical gradients, at the expense of the hydrolysis of one molecule of ATP (*1*). The enzyme consists of an α-subunit (M_r 112 kDa) with 10 transmembrane domains and a large cytoplasmic domain and a *β*-subunit (M_r 35 kDa) with one transmembrane domain. The cytoplasmic domain of the α-subunit can, by analogy to the known structure of the Ca-ATPase (*2*), be subdivided into the N-domain containing the nucleotide binding site, the P-domain containing the phosphorylation site, and the activation A-domain. The binding sites for both Na^+ and K^+ are located in the α-subunit, presumably surrounded by membrane-spanning segments 4−6 and 8 (*3*). Two K^+ ions are occluded by Na,K-ATPase in the E_2-conformation as part of the hydrolysis cycle, whereas the occlusion of Na^+ occurs transiently in the E_1 phosphorylated enzyme conformations (*1*). Scheme 1 outlines the kinetics of the spontaneous K^+-occlusion reaction (*4*).

The E_1-form[1] of the enzyme binds K^+ with an intrinsic low affinity, and a dissociation constant K_K of about 10 mM has been estimated from rapid-mixing stopped-flow fluorescence measurements (*5*). With a diffusion controlled binding rate constant of about 10^8 M^{-1} s^{-1}, the dissociation rate constant for this low-affinity site is about 10^6 s^{-1} (= K_K·10^8 M^{-1} s^{-1}). The low-affinity binding is followed by a spontaneous occlusion of the two K^+ ions and conversion to the E_2-form, that is, a sequestering that prevents rapid exchange with free K^+ ions in solution. The occlusion reaction occurs with a large rate constant (e.g., k_1 ∼300 s^{-1}), whereas deocclusion is described by a very small rate constant k_{-1} of about 0.3 s^{-1} (at room temperature), which can be determined biochemically (for an overview, see ref (*6*)). Thus, the apparent dissociation constant for K^+ (K_{Occ}) is related to K_K by the relationship $K_{Occ} \approx K_K \cdot k_{-1}/k_1$. From this model, it is seen that the two occluded K^+ ions are in slow equilibrium with free K^+, that is, the exchange rate ($k_1 + k_{-1}$) is of the order of 300 s^{-1}. In contrast to this, K^+ bound to nonspecific low-affinity sites (other than those leading to the occlusion of the ions) will be in rapid equilibrium with free K^+, when it is assumed that the binding rate constant for K^+ is diffusion controlled (see above) and an exchange rate of about 10^6 s^{-1} is estimated for nonspecific sites. This difference between the exchange rate of K^+ bound to nonspecific sites and that of occluded K^+ is important for the subsequent analysis of spectroscopy data.

Scheme 1

$$E_1 + 2\,K^+ \underset{\sim 10^6\ s^{-1}}{\overset{\sim 10^8\ M^{-1}\cdot s^{-1}}{\rightleftharpoons}} E_1{\cdot}K_2 \underset{0.3\ s^{-1}}{\overset{300\ s^{-1}}{\rightleftharpoons}} E_2(K_2)$$

Knowledge of the character of the cation binding and the chemical surroundings of the cations in the occlusion sites is crucial for a detailed understanding of the transport of Na^+ and K^+. Mutagenesis experiments and biochemical modification studies have led to identification of amino acids important for the binding process (*7*), but no details on the local chemical environment of the occlusion sites have been accessible through these techniques. Structural studies by X-ray diffraction (XRD) or liquid-state nuclear magnetic resonance (NMR) spectroscopy are not straightforward because of the difficulties in crystallization and the inherent

† This work was supported by the Danish Medical Research Council, the Danish National Research Foundation, the Danish Natural Science Research Council (SNF), the Danish Biotechnological Instrument Centre (DABIC), Aarhus University Research Foundation, and Carlsbergfondet.

* Corresponding author. Tel: +45 8942 2930. Fax: +45 8612 9599. E-mail: me@biophys.au.dk.

‡ Department of Biophysics.

§ Center for Insoluble Protein Structures (inSPIN).

[1] Abbreviations: B_{Non}, capacity for nonspecific cation binding; B_{Occ}, cation occlusion capacity; CDTA, *trans*-1,2,-cyclohexylenedinitrilotetraacetic acid; Δ*ω*, angular frequency difference; E_1, the enzyme form in Na^+; E_2, the enzyme form with occluded cation; K_{Non}, equilibrium dissociation constant for nonspecific binding; K_{Occ}, equilibrium dissociation constant for occlusion; k_1, k_{-1} rate constant; k_{ex}, exchange rate constant; MAS, magic angle spinning; NMR, nuclear magnetic resonance; T_1, longitudinal relaxation time; *τ*, relaxation delay time.

10.1021/bi060642k CCC: $33.50
Published on Web 08/09/2006

slow molecular motion of the large membrane-bound enzyme. Solid-state NMR, however, is not hampered by these effects and may be better suited for such structural investigations of the electronic and nuclear surroundings, that is, the local chemical environment, of NMR-sensitive nuclei including relevant metal ions.

The E_2 conformation is not only formed in the presence of K^+ but also in the presence of its congeners, such as Rb^+, Cs^+, or Tl^+ (Scheme 1). This feature is important for the practical realizability of solid-state NMR on the metal ion as a means to explore the binding of metals to the Na,K-ATPase. ^{39}K has a very low gyromagnetic ratio and a relative large quadrupole moment, which makes it difficult to study (*8*). This applies in particular when considering the very low concentration of the occlusion sites in the Na,K-ATPase membranes. The congeners include the NMR-sensitive nuclei ^{87}Rb, ^{133}Cs, and ^{205}Tl. Among these, the highest NMR sensitivity and the highest binding affinity is associated with ^{205}Tl, which, therefore, appears to be the most attractive nucleus to study. ^{205}Tl is a spin-1/2 nucleus with a gyromagnetic ratio of $15.589 \cdot 10^7$ rad/T·s and a natural abundance of 70.5%. It has two oxidation levels, Tl(I), which is relevant for the monovalent coordinations to Na,K-ATPase, and Tl(III).

Both of these oxidation states are highly sensitive to the chemical environment with isotropic chemical shift ranges of about 3500 ppm for Tl(I) (*9*) and 7000 ppm for Tl(III) (*9*, *10*). Likewise, the size of the ^{205}Tl chemical shift anisotropy is known to be highly dependent on the electronic and nuclear environments of the Tl nucleus. Hinton and coworkers have reported chemical shifts for complexed ^{205}Tl(I) between −700 and 300 ppm (*11*) and chemical shift anisotropies of up to 855 ppm (*12*). Previous NMR studies have demonstrated that the chemical shifts observed by ^{205}Tl NMR may be powerful probes for the investigation of protein binding sites (*13*, *14*) and conformational changes (*15*, *16*). Furthermore, ^{205}Tl longitudinal relaxation times, T_1, have been examined and used as a means to obtain structural information (*17*). However, all previous ^{205}Tl NMR studies on proteins have been performed on relatively small systems for which liquid-state NMR methods allow for an observation of the cation even in cases of tight binding to the occlusion sites.

In this study, the Tl^+ binding at room temperature to Na,K-ATPase membranes from shark rectal gland and pig kidney has been examined using ^{205}Tl solid-state NMR. The spectra are interpreted by means of Tl^+ binding isotherms calculated from equilibrium experiments with radioactive $^{204}Tl^+$. To the best of our knowledge, this is the first time ^{205}Tl solid-state NMR has been applied to a large complex system as the Na,K-ATPase in a native membrane-associated state. For this system, the chemical shifts and the size of chemical shift anisotropy for occluded Tl^+ are unknown a priori. To cover a situation with a relatively low intrinsic sensitivity and a potential of anisotropic shielding while keeping a relatively big sample volume, magic-angle spinning (MAS) experiments were conducted at a relatively low magnetic field (to reduce the effects from anisotropic shielding) using a large rotor with modest spinning speeds.

MATERIALS AND METHODS

Enzyme Preparation. The Na,K-ATPase membranes from shark rectal glands and pig kidneys were prepared as described earlier (*18*, *19*). The specific Na,K-ATPase activities of the purified preparations were about 2000 μmol P_i/mg·h and 1700 μmol P_i/mg·h for shark and kidney enzymes, respectively. The enzyme preparations contained about 2.9 nmol nucleotide binding sites per mg of enzyme. The shark enzyme was stored at a protein concentration of about 20 mg/mL in 20 mM histidine and 25% glycerol (pH 7.0), and the kidney enzyme was stored at a protein concentration of about 4 mg/mL in 20 mM histidine, 250 mM sucrose, and 1 mM EDTA (pH 7.0). Protein concentrations were determined using the Lowry method (*20*, *21*).

Equilibrium Binding Experiments with ^{204}Tl. Na,K-ATPase was diluted 20-fold with 20 mM histidine, 1.3 mM CDTA buffer (pH 6.9 at 20 °C), and centrifuged for 2 h at 100 000*g* and 10 °C. The supernatant was discarded, and the pellet was homogenized in 20 mM histidine and 1.3 mM CDTA buffer to a total volume of approximately 2.7 mL. The protein concentration in the homogenate was typically 11−12 mg/mL. To aliquots of 207 μL of enzyme homogenate were added concentrated solutions of ^{204}Tl (as sulfate salt) to a final volume of 230 μL, to give nominal final Tl^+ concentrations of about 0.01, 0.02, 0.05, 0.07, 0.1, 0.2, 0.5, 0.7, 1, 2, 5, and 10 mM. The actual total Tl^+ concentration in a sample was determined from the radioactivity in 10 μL aliquots (in quadruplicate). Then, 175 μL was transferred to 200 μL Airfuge tubes (Beckman) and centrifuged at 100 000*g* at 18 °C for 1 h. The concentration of unbound Tl^+ was estimated from the radioactivity in 10 μL of the supernatant (also in quadruplicate), and bound Tl^+ was the difference between total and free Tl^+.

Sample Preparation for NMR. The first step is a 40-fold dilution of Na,K-ATPase membranes in a buffer containing 20 mM histidine, 1.3 mM CDTA (pH 6.9 at 20 °C) followed by centrifugation at 100 000*g* for 2 h at 10 °C. This is done to reduce the concentration of glycerol (or sucrose) and traces of chloride and K^+. The removal of chloride is essential to avoid the formation of poorly soluble TlCl. To the pellet was added a small amount of concentrated Tl_2SO_4 solution (and in some experiments, K_2SO_4 as well) followed by gentle homogenization using a pellet pestle motor, and the suspension was transferred to the NMR rotor within 30 min, sufficient time to allow the equilibration of Tl^+ with enzyme. The protein concentration in the NMR rotor is on average 30 mg/mL, which corresponds to a concentration of Tl^+ occlusion sites of about 0.17 mM, calculated from a nucleotide site concentration of 2.9 nmol/mg and assuming 2 Tl^+ occluded per nucleotide site (*22*).

^{205}Tl NMR Experiments. All ^{205}Tl NMR spectra were recorded on a Varian Inova 300 NMR spectrometer (operating at a field strength of 7.1 T, corresponding to a ^{205}Tl Larmor frequency of 173.018 MHz) equipped with a home-built 7 mm double-resonance ^1H-X MAS probe using thin-wall Si_3N_4 rotors (with a volume of 322 μL). The probe was modified from a standard configuration, allowing X frequencies up to ^{31}P (121.4 MHz) to observe ^{205}Tl (173 MHz) under conditions of ^1H decoupling. The single-pulse excitation spectra are acquired using a $\pi/2$ pulse of 5 μs (corresponding to an rf field strength of 50 kHz), 1 s relaxation delay, with

or without ^{1}H decoupling with 47 kHz rf field strength. T_1 relaxation times are measured using a standard inversion−recovery protocol, $(\pi)_x - \tau - (\pi/2)_x$, with delay times τ between 0 and 1 s for Tl^+ in histidine/CDTA buffer and between 0 and 45 ms for Tl^+ in Na,K-ATPase membranes. The ^{205}Tl NMR experiments on Tl^+ in Na,K-ATPase membranes are recorded using MAS with a spinning frequency of 2000 ± 3 Hz. All experiments are performed at ambient temperature (approximately 17 °C). The ^{205}Tl chemical shifts are referenced relative to the signal from Tl_2SO_4 in a 5 mM aqueous solution. In the presence of CDTA, the ^{205}Tl chemical shift is displaced toward low field because of the binding of Tl^+ to CDTA. The displacement depends on the ratio between [free Tl^+] and [TlCDTA], and at a saturating concentration of CDTA, the Tl^+ resonance is at about 200 ppm (data not shown). At the [Tl^+] used in the present experiments, the resonance from Tl^+ in the aqueous solution is typically at 8−12 ppm, cf. the sharp peak in Figure 2D and E.

Translation of signal intensities (i.e., integrals) into absolute amounts of Tl^+ is obtained by comparing integrals (obtained using the Varian VNMR software after baseline correction) with those obtained for a series of aqueous samples with Tl^+ in different, well-specified concentrations.

Spectra at low concentrations of Tl^+ in Na,K-ATPase membranes are typically recorded over 1−3 days. More than 60% of the specific Na,K-ATPase activity could typically be recovered after an NMR experiment. We did not determine Tl^+ occlusion after the NMR experiments. However, because the occlusion property of Na,K-ATPase is much more robust toward denaturation than overall Na,K-ATPase activity, we are confident that the recorded NMR signals are representative of Tl^+ interactions with native occlusion sites in the enzyme.

During the NMR experiments, the ion may be submitted to a number of chemical exchange processes. The appearance of the spectrum depends on the relationship between the exchange rate k_{ex} ($= k_1 + k_{-1}$) and the angular frequency difference, $\Delta\omega$, between the resonances corresponding to the two isolated states ($\Delta\omega = \gamma B_0 \Delta\delta$, where γ is the gyromagnetic ratio, B_0 the external magnetic field, and $\Delta\delta$ is the chemical shift difference between the two states). When the rate of exchange is much slower, two discrete peaks appear at the positions corresponding to the NMR chemical shifts of the two states. The broadening of resonances is $k_{ex}(1 - p)$, where p is the relative population of that state. When the rate of exchange is much faster, one signal appears at a position that is the population weighted average of the two states and with a line broadening of $p(1 - p)(\Delta\omega)^2/k_{ex}$. Between these two regimes, the full Bloch−McConnell equations can be used to evaluate the data (*23*, *24*).

RESULTS

Tl^+ Binding to Na,K-ATPase Membranes. Quantitative interpretation of the NMR spectra of Tl^+ interacting with Na,K-ATPase membranes requires well-determined binding constants for Tl^+. Figure 1 shows the results of equilibrium Tl^+-binding experiments for Na,K-ATPase from both shark rectal gland and pig kidney membranes. The experiments are performed by the addition of Tl^+ to the membranes followed by the separation of bound and free Tl^+ by centrifugation (see Materials and Methods). In the low concentration range, binding with high affinity, interpreted as binding to occlusion sites (see below), is observed. At higher Tl^+ concentrations, a considerable amount of lower-affinity nonspecific binding sites is observed.

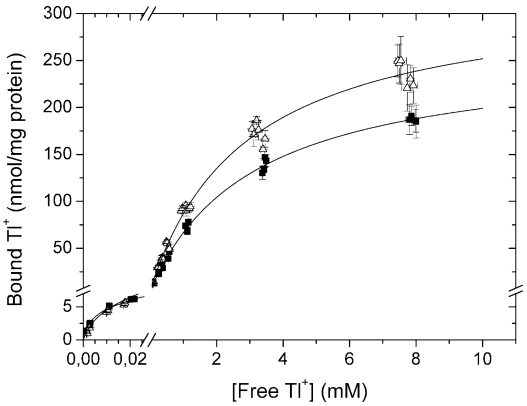

FIGURE 1: Equilibrium binding measurements with $^{204}Tl^+$ in Na,K-ATPase from shark rectal gland (■) and pig kidney (△). The experiments were performed at 20 °C at pH 6.9 in a 20 mM histidine and 1.3 mM CDTA buffer with protein concentrations of about 10 mg/mL and Tl^+-concentrations between 10 μM and 10 mM (see Materials and Methods). The lines represent fitting to eq 1 (see text). Note the expanded scale in the μM range.

The equilibrium binding data of Figure 1 are fitted to a sum of two terms. The first hyperbolic term describes Tl^+ binding to the occlusion sites, with a capacity B_{Occ} and a dissociation constant K_{Occ}. The nonspecific binding to the membranes is fitted by an additional hyperbolic term:

$$[\text{bound } Tl^+] = B_{Occ} \cdot [Tl^+]/(K_{Occ} + [Tl^+]) + B_{Non} \cdot [Tl^+]/(K_{Non} + [Tl^+]) \quad (1)$$

This two-component model is applicable in the Tl^+ range shown in Figure 1 and is used to estimate the relative amounts of occluded, nonspecifically bound, and free Tl^+ detected in the NMR experiments.

The binding of Tl^+ ions to the occlusion sites with high affinity is seen in the expanded part of the graph at the lowest Tl^+ concentrations. In separate experiments using a cation-exchanger technique (*25*), the dissociation constants for the occlusion sites are determined as $K_{Occ} = 6.1 \pm 1.9$ μM for shark and $K_{Occ} = 4.6 \pm 1.4$ μM for kidney Na,K-ATPase (data not shown). These values are used in the fitting procedure for the data in Figure 1 to obtain the occlusion capacities $B_{Occ} = 5.3 \pm 1.3$ nmol/mg for shark Na,K-ATPase and $B_{Occ} = 5.6 \pm 1.0$ nmol/mg for kidney Na,K-ATPase. These values are in good agreement with the expected occlusion capacity of 2 Tl^+ per protein molecule (the concentration of shark and kidney enzymes measured as the concentration of nucleotide sites were both about 2.9 nmol/mg), and the dissociation constants are as those reported earlier for the kidney enzyme (*22*).

The dissociation constant for nonspecific binding is $K_{Non} = 3.1 \pm 0.26$ mM with a large number of binding sites $B_{Non} = 260 \pm 40$ nmol/mg for shark Na,K-ATPase. The corresponding values for kidney Na,K-ATPase are $K_{Non} = 2.9 \pm 0.40$ mM and $B_{Non} = 310 \pm 50$ nmol/mg, respectively. The affinities of the nonspecific Tl^+ binding sites are thus similar, whereas the kidney enzyme contains a somewhat larger number of sites per mg of protein.

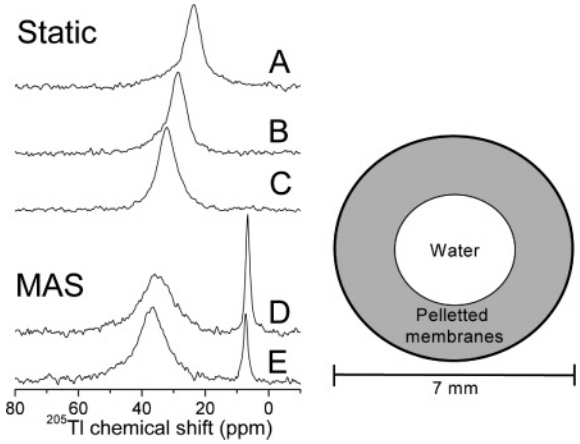

FIGURE 2: ^{205}Tl static and MAS NMR experiments of Na,K-ATPase membranes. Left panel: ^{205}Tl NMR spectra of 10 mM Tl^+ in Na,K-ATPase membranes from shark rectal glands. (A−C) Static ^{205}Tl NMR spectra recorded without sample spinning at protein concentrations of 10 (A), 20 (B), and 30 mg/mL (C). (D) Same sample as (C) recorded under 2 kHz MAS conditions. (E) Re-recording of (D) after the removal of about 50 μL of water from the water phase from the center of the rotor. Right panel: Cartoon of the MAS rotor seen from above, illustrating the separation of the sample into an aqueous phase and a membrane phase during spinning.

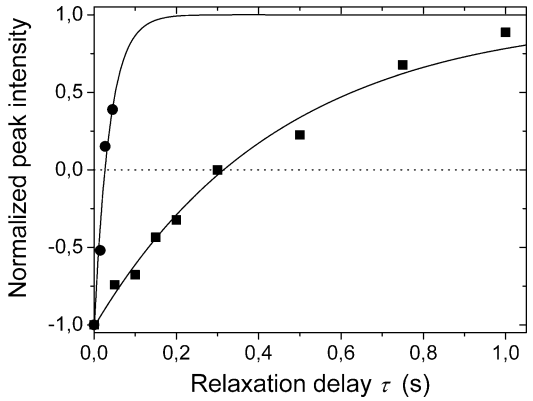

FIGURE 3: T_1 relaxation experiments. The ^{205}Tl NMR inversion recovery experiments were done with 50 mM Tl^+ in buffer (20 mM histidine and 1.3 mM CDTA at pH 6.9 at 17 °C) and with 1.5 mM Tl^+ added to Na,K-ATPase membranes at 40 mg protein/mL in the same buffer. The normalized peak intensities are shown for Tl^+ in buffer (■) and with enzyme (●). The lines represent the best fit to the relationship $M(\tau) = 1-2e^{-\tau/T_1}$, where M is the normalized peak intensity, τ is the relaxation delay time, and T_1 is the longitudinal relaxation time (*38*). T_1 deduced from this analysis is 501 ms for Tl^+ in buffer and 38 ms for Tl^+ with enzyme.

Sample Morphology during Magic-Angle Spinning NMR. Magic-angle-spinning (2 kHz) of the membrane sample leads to a physical separation into an aqueous phase, residing in the center of the rotor, and a membranous phase along the rotor wall as visualized in Figure 2 (right panel). Typical ^{205}Tl NMR spectra of membranes equilibrated with 10 mM Tl^+ are shown to the left in Figure 2. When a static (i.e., no sample spinning) spectrum is recorded, a broad asymmetric peak at 20−30 ppm is observed (Figure 2A−C). The resonance position of the peak is shifted downfield as the protein concentration is increased from 10 mg/mL (Figure 2A) to 30 mg/mL (Figure 2C). After spinning the latter sample under MAS conditions for 30 min, the ^{205}Tl NMR signal is split into two clearly separated components, one at about 8 ppm and the other in the 30−50 ppm range (Figure 2D). Part of the aqueous phase in the center can subsequently be removed using a Hamilton syringe. Re-recording the spectrum now reveals a reduction in the resonance at 10 ppm (Figure 2E), showing that this signal is due to aqueous Tl^+ in the center of the rotor.

Under MAS conditions, the enzyme along the rotor wall experiences an acceleration of 48 000*g* corresponding to a pressure of 13.7 bar (the inner radius of the rotor is 2.95 mm). This pressure on the membranous layer is well below the critical value of about 200 bar, above which the enzyme may denature irreversibly (*26*). The water phase in the middle of the rotor accounts for approximately one-third of the total volume of the sample in the rotor. The protein concentration in the membrane layer is estimated to be about 50 mg/mL from control experiments where the pellet after centrifugation under similar conditions is collected and analyzed for protein content. In agreement with this, the resonance position under MAS conditions is shifted further downfield relative to the static experiments (compare Figure 2C with D and E).

The static spectra with 10 mM Tl^+ (Figures 2A−C) have the same overall line shape for protein concentrations from 10 to 30 mg/mL. With 10 mg/mL, about 2.0 mM of the Tl^+ is bound, increasing to 3.8 mM at 20 mg/mL and to 4.8 mM with 30 mg protein/mL (calculated using eq 1). The free and bound Tl^+ do not appear as separate peaks, but both contribute to a single peak, the chemical shift of which increases with the protein concentration (from about 24 to 32 ppm). This suggests that free and bound Tl^+ are in fast exchange (much faster than ~30 000 s^{-1}), with chemical shifts of the free and bound states of about 18 and 46 ppm, respectively, as estimated from the protein concentration dependence of the observed chemical shift. This means that free Tl^+ is perturbed by membrane suspension, leading to a low-field shift of the resonance relative to the shift in the water phase of about 10 ppm.

Relaxation Experiments. The longitudinal relaxation behavior of Tl^+ in buffer solution was compared with that of Tl^+ bound to the Na,K-ATPase membranes in Figure 3. For 50 mM Tl^+ in buffer, a series of relaxation experiments was performed with delay-times from 0 to 1000 ms, resulting in a longitudinal relaxation time, T_1, of 501 ms (Figure 3). Relaxation experiments with 1.5 mM Tl^+ in equilibrium with Na,K-ATPase membranes were done at a protein concentration of about 40 mg protein/mL, giving a Tl^+/enzyme ratio of about 11 mol/mol. The T_1 for Tl^+ bound to the membranes is about 38 ms (Figure 3), which is considerably shorter than the value of 501 ms deduced for free Tl^+. The shorter T_1 is an effect of slower correlation time and increased dipolar interactions due to protein and/or membrane binding. In the following sections, the analysis of the distribution of Tl^+ between the aqueous phase and the occluded as well as nonspecific sites takes this difference in relaxation rates into account. This is necessary because the relaxation delay employed in the MAS experiments was 1 s, sufficient to allow the full recovery of Tl^+ bound to membranes but only about 80% recovery of the free Tl^+ in buffer.

MAS NMR Experiments with Tl^+ at Stoichiometric Concentrations. ^{205}Tl MAS NMR spectra of Tl^+ in shark rectal gland Na,K-ATPase membranes are shown in Figure 4, where the effects of proton decoupling as well as the displacement of bound Tl^+ by K^+ are reported. Figure 4A shows a spectrum without proton decoupling and about 9

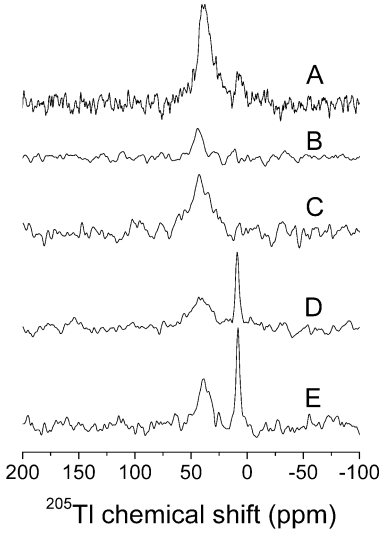

FIGURE 4: ^{205}Tl MAS NMR spectra of Tl^+ interacting with Na,K-ATPase from shark rectal glands. In all five samples, the protein concentration was about 30 mg/mL in the rotor. For experiment (A), the sample contains about 9 mol Tl^+ per mol enzyme, and the integrated intensity corresponds to about 7 mol Tl^+ per mol enzyme. In experiments (B−E), the sample contains 3.3 mol Tl^+ per mol enzyme. For experiment B, the integrated intensity corresponds to about 0.8 mol Tl^+ per mol enzyme. Experiment C is identical to B, except that ^1H decoupling was employed during data collection, and the integrated intensity was 3.2 mol Tl^+ per mol enzyme. Experiments D and E are similar to B and C but with the addition of a 100-fold excess of K^+ (330 mol K^+ per mol enzyme). The integrated signal intensities correspond to 2.9 (D) and 3.4 mol Tl^+ per mol enzyme (E). The experiments are performed at 17 °C at pH 6.9 in a 20 mM histidine and 1.3 mM CDTA buffer. Spectra B−E have the same vertical scale, and spectrum A has been reduced 2.2-fold in order to ease comparison.

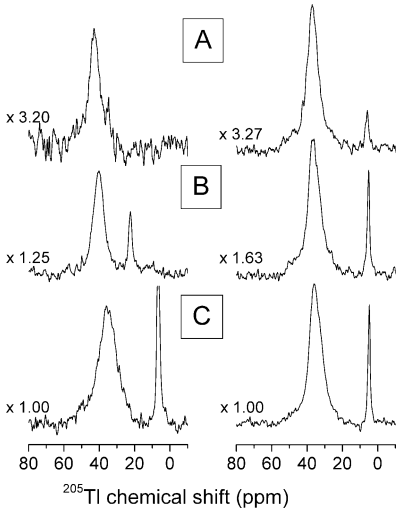

FIGURE 5: ^{205}Tl MAS NMR spectra of Tl^+ nonspecifically bound to Na,K-ATPase. The experiments shown in the left panel are with shark rectal gland Na,K-ATPase at 17 °C at pH 6.9 in a 10 mM histidine and 0.67 mM CDTA buffer with about 30 mg protein/mL in the rotor and Tl^+ concentrations of 2 (A), 5 (B), and 10 mM (C). Similar experiments are shown in the right panel with Na,K-ATPase from pig kidney with Tl^+ concentrations of 2 (A), 5 (B), and 10 mM (C). The vertical scale of spectra A and B have been expanded relative to spectrum C with factors shown to ease comparison.

mol Tl^+ per mol of enzyme. However, only about 7 mol/mol can be accounted for by integration of the intensity of Tl^+ in the spectral range shown. At a lower, almost stoichiometric Tl^+ concentration of 3.3 mol Tl^+ per mol of enzyme, only about 0.8 mol Tl^+/mol enzyme is detectable (Figure 4B). This indicates that resonances from the remaining fraction of Tl^+ (2.5 mol/mol) may be too broad to permit detection under these experimental conditions. One possible explanation is that the occluded Tl^+ (2 mol/mol enzyme) is sufficiently tightly bound to the enzyme for anisotropic nuclear spin interactions, such as chemical shift anisotropy or dipole−dipole coupling to surrounding spins, to broaden the resonance beyond detection.

To explore the effect of $^1H-^{205}Tl$ dipolar coupling interactions in the occlusion site of Na,K-ATPase, a ^{205}Tl NMR spectrum was recorded using the same conditions except that ^1H decoupling was applied. As shown in Figure 4C, a more intense signal was observed, corresponding to a total of about 3 mol Tl^+ per mol of enzyme, that is, in principle, all of the added Tl^+. On average of four experiments, the signal increase induced by proton decoupling corresponded to about 1.3 mol of Tl^+ per mol of enzyme. The resonances from the two occluded Tl^+ contribute to the peak at about 40 ppm (Figure 4C). It is interesting to note that this chemical shift is very similar to that observed without proton decoupling (Figure 4B). Furthermore, it is noteworthy that the signal does not display clearly distinguishable signs of anisotropic chemical shielding, which typically leads to a manifold of spinning sidebands. The presence of a sideband pattern could not, however, be verified by experiments with different spinning frequencies, indicating that the broadening to a large extent is inhomogeneous and most likely is dominated by a distribution of different isotropic chemical shifts from sites with slightly different electronic environments for Tl^+ influenced by motion or exchange with the surroundings.

In the presence of a 100-fold excess of K^+, practically all of the Tl^+ is visible, both in the absence (Figure 4D) and presence (Figure 4E) of ^1H decoupling. Integration of the spectrum recorded with and without ^1H decoupling (Figure 4D and E) gives about 2.8 mol Tl^+ in the membrane phase and about 0.3−0.4 mol Tl^+ for the aqueous signal at 10 ppm. The affinity for binding to the occlusion sites of the enzyme is about 8 times larger for Tl^+ than that for K^+ (L. O. Jakobsen, unpublished result). A 100-fold excess of K^+ should, therefore, release more than 90% of the occluded Tl^+. It should be noted that the resonance line width for the signal from nonoccluded Tl^+ in the membrane phase appears to be slightly smaller than that observed for occluded Tl^+.

NMR Characterization of Nonspecific Binding of Tl^+. The nonspecific binding of Tl^+ to Na,K-ATPase membranes was further characterized by ^{205}Tl MAS NMR as shown in Figure 5. These spectra (shown for shark rectal gland enzyme in the left panel and for pig kidney enzyme in the right panel) are recorded with a final Tl^+ concentration in the rotor of 2−10 mM. As the spectra are recorded without ^1H decoupling, the signals from the two occluded Tl^+ per enzyme molecule are not detected. Accordingly, the broad resonance corresponding to Tl^+ in the membrane phase reflects Tl^+ nonspecifically bound to the membranes in equilibrium with free Tl^+ trapped in the water phase between the membranes.

For Tl^+ bound to the shark enzyme, the membrane phase chemical shift decreases from 42 to 35 ppm, and the line shape broadens from about 1.2 to 2.1 kHz upon an increase in Tl^+ from 2 to 10 mM. With a total Tl^+ concentration of

2 mM, the amount of Tl^+ bound to the protein is about 1.61 mM (calculated using eq 1 with the values for the parameters K_{Non} and B_{Non} given above and assuming that the protein concentration in the membrane phase is about 50 mg/mL). The broad peak observed for shark enzyme in Figure 5A is thus predominantly due to the approximately 80% bound Tl^+, with only about 20% being free (but in the membrane phase). With 5 and 10 mM Tl^+, the fractions of bound Tl^+ decrease to 76% and 68%, respectively.

For Tl^+ bound to the kidney enzyme, the membrane phase chemical shift decreases considerably less than that for shark enzyme, from 36.6 to 34.9 ppm, and the line shape broadens from 1.27 to 1.42 kHz upon an increase in Tl^+ from 2 to 10 mM, cf. Figure 5, right panel. The fraction of bound Tl^+ decreases from about 84% at 2 mM total Tl^+ to about 72% at 10 mM Tl^+.

DISCUSSION

Properties of Occluded Tl^+. It is well established that 2 Tl^+ ions are occluded in Na,K-ATPase during the catalytic cycle (*27*) and that the spontaneous deocclusion rate constant is small, about 0.3 s^{-1} (*28*). Thus, Tl^+ is a suitable congener for K^+ for analysis of the properties of the occlusion site in the E_2-form. The high apparent affinity for Tl^+ (K_{Occ} in the μM range) is favorable for the present type of experiments, allowing for an almost stoichiometric binding of Tl^+ to the occlusion sites with only a low amount of binding to nonspecific sites. In the NMR experiments, the signal from the occluded ^{205}Tl can be detected when proton decoupling, which suppresses the dipole−dipole interactions between Tl^+ and the surrounding protons, is applied. Under these conditions, the signal increases relative to that in experiments without decoupling by an amount that roughly corresponds to the amount of occluded Tl^+ sites so that most of the Tl^+ in the sample is accounted for.

This observation indicates that ^{205}Tl may form relatively strong dipole−dipole couplings with protons in the binding sites. Taking the Ca-ATPase structure as a model (*3*), the shortest distance between bound Ca^{2+} and one of the protons on C_β in Thr799 is about 2.4 Å, corresponding to a $^1H-^{205}Tl$ dipole−dipole coupling $b_{HTl}/2\pi = -\gamma_H\gamma_{Tl}\mu_0\hbar\langle 1/r_{TlH}^3\rangle/8\pi^2$ of about 5 kHz (γ_H and γ_{Tl} are the gyromagnetic ratios of ^1H and ^{205}Tl, μ_0 is the permeability of free space, $\hbar$ is Planck's constant divided by 2π, and r_{TlH} is the Tl−H distance). In this view, the effect of ^1H decoupling on the spectra indicates that the occluded Tl^+ ions are somewhat restricted in their mobility in the binding pocket, otherwise the $^1H-^{205}Tl$ dipolar couplings would be averaged out, and ^1H decoupling would have no effect. An approximate estimate of the residence time in the site can be obtained by assuming an isotropic tumbling motion of the Tl^+ within the Redfield limit (the motions are much faster than the angular frequency of the interaction) (*29*), and a line width, $\Delta\nu_{1/2}$, in the range of 5 kHz is necessary to broaden the signal beyond detection. Thus, a lower limit of about half a ms for the correlation time τ_{cor} for isotropic tumbling of the Tl^+ is obtained using $\tau_{cor} = 5\pi\Delta\nu_{1/2}/b_{HTl}^2$ (*30*). Although the correlation time obtained is not within the Redfield limit and, therefore, should be considered very approximate, this indicates that the ions are quite rigidly bound and not merely enclosed in the sites when occluded.

The dipole−dipole coupling between the two ^{205}Tl atoms may also influence the NMR spectra. If the Tl^+-Tl^+ distance in Na,K-ATPase is similar to the $Ca^{2+}-Ca^{2+}$ distance in Ca-ATPase of 5.7 Å (*2*), then a homonuclear dipole−dipole coupling of $b_{TlTl}/2\pi = -220$ Hz is obtained. With a line width of approximately 3.5 kHz, a dipolar interaction of this size may contribute to part of the line broadening, although it cannot be determined or discriminated from other effects in the present spectra.

^{205}Tl is typically associated with a large chemical shift anisotropy in asymmetric environments. The signal from the occluded Tl^+ appears to be fairly isotropic (i.e., no sidebands reflecting chemical shielding anisotropy; see above), which may suggest fast motion relative to the time scale of the NMR experiment, or high symmetry of the donor atoms relative to Tl^+. The broad resonance may, in principle, cover a broadened/nonresolved spinning sideband pattern reflecting chemical shielding anisotropies up to about 25 ppm. This is almost negligible compared to the anisotropies of hundreds of ppm previously reported for valinomycin and gramicidin complexes (*11*, *12*). This could indicate that Tl^+ is quite symmetrically located with respect to the surrounding donor atoms or that occluded Tl^+ ions are not very tightly bound within the occlusion sites. However, if one assumes that contributions to the line shape from the anisotropic terms of the dipolar coupling and chemical shielding scale with the correlation time are in the same way as that within the Redfield limit (*29*) and that the entire 3.5 kHz line width stems from anisotropic shielding, an upper limit for chemical shielding anisotropy Δ_σ of about 60 ppm is obtained using $\Delta_\sigma = -3\nu_\sigma^{aniso}/(2\nu_0)$ with $\nu_\sigma^{aniso} = \sqrt{5\Delta\nu_{1/2}/(4\pi\tau_{cor})}$ (ν_0 is the Larmor frequency of ^{205}Tl) (*30*). This indicates that the environment of Tl^+ is highly symmetric.

The above considerations are based on the assumption that the protein is rigidly bound in the membranes. However, this is not necessarily the case. Electron paramagnetic spectroscopic studies of spin-labeled Na,K-ATPase show rotational correlation times about the membrane normal on the order of 10−30 μs (*31*). Motions at this time scale would significantly decrease the detectable effects of dipole−dipole couplings and chemical shift anisotropy components perpendicular to the membrane normal. The upper limit of about 60 ppm for Δ_σ would then only account for the chemical shift anisotropy component parallel to the membrane normal.

Because the signal from the nonspecifically bound and free Tl^+ is visible in the absence of proton decoupling, the exchange between the occlusion sites and the nonspecific sites must be slow on the chemical shift time-scale, that is, $k_{ex} \ll 2\pi\nu_0\Delta\delta$, where k_{ex} is the exchange rate, and $\Delta\delta$ is the chemical shift difference between the two states. Even a chemical shift difference as small as 0.01 ppm, giving an exchange rate significantly slower than 10 s^{-1}, agrees well with the previously measured rate of deocclusion of 0.17 s^{-1} (*28*).

Surprisingly, the almost identical chemical shifts for the occlusion and nonspecific sites suggests that the electronic environments of Tl^+ under these conditions are quite similar. We should note, however, that the relatively broad resonance (20−30 ppm) may account for an inhomogeneous distribution of sites with slightly different electronic surroundings. The isotropic chemical shift of the occluded ^{205}Tl is about

45 ppm. This is somewhat lower than the shift of about 127 ppm observed for the antibiotics lasalocid and nigericin, which have one coordinating carboxylate and two hydroxyls, and the shift of 107 ppm observed for monensin with Tl coordinating to two hydroxyls (*11*, *12*). However, it is much higher than that for nonactin and valinomycin, which use only carbonyls and esters to coordinate the ion and have ^{205}Tl shifts below −261 ppm (*11*). The chemical shift does suggest occlusion sites with something similar to a single carboxylate or hydroxyl ligand together with a number of carbonyls. Interestingly, this is neither in agreement with the ligands suggested for K^+ site I in a model made from Ca-ATPase by Ogawa and Toyoshima (*3*), which contains three carboxylates and one hydroxyl, nor with the model for K^+ site II, which contains two carboxylates. It is also not in agreement with a site consisting of only backbone carbonyls such as in the KcsA K^+ channel (*32*). One could rather imagine environments such as those in the K^+-site on Ca^{2+}-ATPase (*33*) with three backbone oxygens, a single side chain carboxylate, and two waters, maybe with the exception of the waters. Such ligands would also be in accordance with the fact that K^+ does not share the preference for charged ligands of Ca^{2+} (*34*).

Nonspecific Tl^+ Binding Characterized with NMR. In the absence of ^{1}H decoupling, the ^{205}Tl MAS NMR spectrum of Na,K-ATPase with a small excess of Tl^+ relative to the occlusion sites shows no signal from the occluded Tl^+. Only the 1.3 mol Tl^+ in excess of the occlusion sites produces a small signal at about 40 ppm (Figure 4B). If an excess of K^+ is added, the occluded Tl^+ is displaced, and there is an increase in the ^{205}Tl signal so that almost all Tl^+ is now observed (Figure 4D). These observations suggest that all of the nonoccluded Tl^+ can be accounted for by the signals observed in the NMR spectra without ^{1}H decoupling and that the nonoccluded Tl^+ cations are mobile and not tightly attached to either the protein or membranes on the time scale of the NMR experiment. ^{1}H decoupling has no significant effect on the spectra with excess K^+, indicating that nonspecifically bound Tl^+ does not form strong dipolar couplings with the protons as discussed above. The displacement of Tl^+ from the occlusion sites by K^+ also increases the concentration of free Tl^+, which is reflected in the appearance of a peak at about 10 ppm (Figure 4). The slight movement of the ^{205}Tl signal from the membrane phase relative to the spectra in the absence of K^+ is likely a consequence of fast exchange between nonspecifically bound and free ^{205}Tl, identical to the ^{205}Tl reported for the water-phase signal. The chemical shift difference between these two states on the order of 10−20 ppm implies that the exchange rate is much larger than 10 000 s^{-1}.

The ^{205}Tl NMR spectra in Figure 5 show Tl^+ bound to nonspecific sites in Na,K-ATPase membranes from a shark rectal gland (Figure 5, left panel) and a pig kidney (Figure 5, right panel). The signal at around 40 ppm represents an average of the signals from ^{205}Tl in various nonspecific sites and free in solution. This is due to fast exchange between these different locations. At 2 mM Tl^+, more than 80% of the Tl^+ is bound to the enzyme (cf. Figure 1 and eq 1), and the signal is dominated by contributions from nonspecifically bound Tl^+. As the fraction of bound Tl^+ decreases to about 76% at 5 mM Tl^+ and about 68% at 10 mM Tl^+, the contribution from free Tl^+ increases, and the signal corresponding to the membrane phase decreases in chemical shift. As noted above in relation to Figure 2, the free Tl^+ in the membrane phase must have a higher chemical shift than free Tl^+ in the buffer in the middle of the rotor because the peak position should be a population-weighted average between the signals corresponding to the two exchanging states. However, the shift of ^{205}Tl is very sensitive to solvent conditions (*9*); therefore, even minor differences in the environment of the free Tl^+ in the membrane and water phases can lead to the observed changes in the shift of free Tl^+.

The resonance position and line width of Tl^+ bound to shark membranes changes with the Tl^+ concentration more markedly than Tl^+ bound to the kidney enzyme (Figure 5). This may reflect different Tl^+ exchange rates between the pellet and water phase for the two enzymes, with slow exchange (much slower than ∼17 000 s^{-1}) for kidney and intermediate exchange (somewhat slower than ∼17 000 s^{-1}) for shark enzyme.

A factor contributing to this variation could be a difference between the morphology of the membrane pellets of shark and kidney enzymes. When pelleted by centrifugation under otherwise identical conditions, the kidney membranes form a more dense and tightly packed pellet than the more viscous shark membranes (M. Esmann, unpublished observation). This finding agrees favorably with the suggested slow exchange of Tl^+ between the water and membrane phases in the kidney and the intermediate exchange in the shark; the more dense pellet results in a slower exchange of ions with the surroundings (see above). A consequence of these considerations is that although the appearance of the signal corresponding to Tl^+ in the membrane phase differs between shark and kidney enzyme at 2−10 mM Tl^+, this is most likely related to the exchange properties of unbound Tl^+ and not to differences in the spectral properties on the nonspecifically bound Tl^+. The presented data, therefore, suggest that the nonspecific Tl^+ sites over a wide range of [Tl^+] have similar properties, both for shark and kidney Na,K-ATPase.

At present, the functional relevance of the nonspecific cation sites is not clear. The large number of nonspecific sites, about 280 nmol/mg of protein equivalent to about 90 mol/mol, could be formed around negatively charged aspartate and glutamate residues of which there are 126 per α-subunit of the shark rectal gland Na,K-ATPase (GenBank accession number AJ781093). From homology modeling with Ca-ATPase, it is inferred that more than half of these are on the surface of the protein and that there is, thus, good agreement between the binding capacity (Figure 1) and the potential of the negatively charged binding sites. From kinetic experiments, Askari and co-workers (*35*) have suggested cation binding to access channels leading to the occlusion sites. These sites cannot be spectrally resolved with the ^{205}Tl MAS NMR technique. Grisham et al. (*36*) suggested a Tl^+ site close to the nucleotide binding site on Na,K-ATPase from relaxation experiments. From our data, we cannot resolve such a site (which would appear with only half of the intensity of the occluded Tl^+), but it could be part of the large group of nonspecific sites. However, it should be noted here that the average affinity of around 3 mM of this group of sites is stronger than the 16 mM estimated for Tl^+ binding to the water-filled cavity at the entrance of the KcsA K^+ channel (*37*).

Because ^{205}Tl is a very sensitive NMR nucleus with a vast range of chemical shifts and chemical shift anisotropies, it was expected a priori that the spectra would consist of a number of different resonances according to different Tl^+ surroundings, more or less broadened or split into spinning sidebands by anisotropic interactions, such as chemical shift anisotropy and dipolar couplings. However, as discussed above, the Tl^+ ions bound in these sites appear to be in fast exchange with the solvent and, thus, also between the different types of sites. The detected chemical shifts, therefore, represent only population averages of the involved sites, and we have not, bearing the above-mentioned methodological caveats in mind, attempted a more detailed analysis of the present data set.

CONCLUSION

We have, for the first time, explored the use of ^{205}Tl solid-state NMR for the characterization of the binding of Tl^+-ions to Na,K-ATPase membranes from both shark rectal glands and pig kidneys. Using this technique in combination with biophysical measurements, it has been demonstrated that the signal from occluded and nonspecifically bound Tl^+ can be detected and distinguished by NMR. Effects of dipole−dipole coupling between ^1H and ^{205}Tl in the occlusion sites show that the ions at room temperature are rigidly bound, rather than just occluded. Furthermore, a relatively low isotropic chemical shift suggests occlusion sites with small contributions from carboxylate and hydroxyl ligands.

ACKNOWLEDGMENT

The excellent technical assistance of Ms. Angelina Damgaard, Ms. Birthe Bjerring Jensen, and Ms. Anne Lillevang is acknowledged. We thank Professor H. J. Jakobsen for access to the Varian Unity 300 spectrometer, Mr. P. Daugaard for assistance with modifications of the MAS probe, and Dr. Philippe Champeil for helpful discussions. We also thank the reviewers for very detailed comments and suggestions for improvement.

REFERENCES

1. Glynn, I. M. (1985) The Na^+, K^+-Transporting Adenosine Triphosphatase, in *Enzymes of Biological Membranes* (Martonosi, A., Ed.) 3rd ed., pp 35−114, Plenum Publishing Company, New York.
2. Toyoshima, C., Nakasako, M., Nomura, H., and Ogawa, H. (2000) Crystal structure of the calcium pump of sarcoplasmic reticulum at 2.6 Å resolution, *Nature 405*, 647−655.
3. Ogawa, H., and Toyoshima, C. (2002) Homology modelling of the cation binding sites of Na^+K^+-ATPase, *Proc. Natl. Acad. Sci. U.S.A. 99*, 15977−15982.
4. Karlish, S. J. D., and Stein, W. D. (1982) Protein conformational changes in (Na,K)-ATPase and the role of cation occlusion in active transport, *Ann. N.Y. Acad. Sci. 402*, 226−238.
5. Steinberg, M., and Karlish, S. J. D. (1989) Studies on conformational changes in Na, K-ATPase labeled with 5-iodoacetamidofluorescein, *J. Biol. Chem. 264*, 2726−2734.
6. Glynn, I. M., and Karlish, S. J. D. (1990) Occluded cations in active transport, *Annu. Rev. Biochem. 59*, 171−205.
7. Toustrup-Jensen, M., and Vilsen, B. (2003) Functional consequences of alterations to Ile279, Ile283, Glu284, His285, Phe286, and His288 in the NH2-terminal part of transmembrane helix M3 of the Na^+,K^+-ATPase, *J. Biol. Chem. 278*, 36653−36664.
8. Larsen, F. H., Skibsted, J., Jakobsen, H. J., and Nielsen, N. C. (2000) Solid-state QCPMG NMR of low-g quadrupolar nuclei in natural abundance, *J. Am. Chem. Soc. 122*, 7080−7086.
9. Hinton, J. F., Metz, K. R., and Briggs, R. W. (1988) Thallium NMR spectroscopy, *Prog. Nucl. Magn. Reson. Spectrosc. 20*, 423−513.
10. Aramini, J. M., Krygsman, P. H., and Vogel, H. J. (1994) Thallium-205 and carbon-13 NMR studies of human sero- and chicken ovotransferrin, *Biochemistry 33*, 3304−3311.
11. Hinton, J. F., Metz, K. R., and Millet, F. S. (1981) A thallium-205 NMR study of the thallium(I)-valinomycin complex in the solid state, *J. Magn. Reson. 44*, 217−219.
12. Hinton, J. F., Metz, K. R., Turner, G. L., Bennet, D. L., and Millet, F. S. (1985) A solid-state ^{205}Tl NMR study of the Tl^+-lasalocid- and Tl^+-gramicidin complexes, *J. Magn. Reson. 64*, 120−123.
13. Markham, G. D. (1986) Characterization of the monovalent cation activator binding site of S-adenosylmethionine synthetase by ^{205}Tl NMR of enzyme-bound Tl^+, *J. Biol. Chem. 261*, 1507−1509.
14. Bertini, I., Luchinat, C., and Messori, L. (1983) Tl-205 as an NMR probe for the investigation of transferrin, *J. Am. Chem. Soc. 105*, 1347−1350.
15. Loria, J. P., and Nowak, T. (1998) Conformational changes in yeast pyruvate kinase studied by $^{205}Tl^+$ NMR, *Biochemistry 37*, 6967−6974.
16. Susan-Resiga, D., and Nowak, T. (2003) Monitoring active site alterations upon mutation of yeast pyruvate kinase using $^{205}Tl^+$ NMR, *J. Biol. Chem. 278*, 40943−40952.
17. Hill, K. A. W., and Castellino, F. J. (1987) Topographical relationships between the monovalent and divalent cation binding sites of des-1-41-light chain bovine plasma protein C and des-1-41-light chain-activated bovine plasma protein C, *J. Biol. Chem. 262*, 7105−7108.
18. Jørgensen, P. L. (1974) Purification and characterization of (Na^+ plus K^+)-ATPase. 3. Purification from the outer medulla of mammalian kidney after selective removal of membrane components by sodium dodecylsulphate, *Biochim. Biophys. Acta 356*, 36−52.
19. Skou, J. C., and Esmann, M. (1979) Preparation of membrane-bound and of solubilized ($Na^+ + K^+$)-ATPase from rectal glands of *Squalus acanthias*. The effect of preparative procedures on purity, specific and molar activity, *Biochim. Biophys. Acta 567*, 436−444.
20. Lowry, O. H., Rosebrough, N. J., Fahr, A. L., and Randall, R. J. (1951) Protein measurement with the Folin phenol reagent, *J. Biol. Chem. 193*, 265−275.
21. Peterson, G. L. (1977) A simplification of the protein assay method of Lowry et al. which is more generally applicable, *Anal. Biochem. 83*, 346−356.
22. Jensen, J., and Nørby, J. G. (1989) Thallium binding to native and radiation-inactivated Na^+/K^+-ATPase, *Biochim. Biophys. Acta 985*, 248−254.
23. McConnell, H. M. (1958) Reaction rates by nuclear magnetic resonance, *J. Chem. Phys. 28*, 430−431.
24. Palmer, A. G., III, Kroenke, C. D., and Loria, J. P. (2001) Nuclear magnetic resonance methods for quantifying microsecond-to-millisecond motions in biological macromolecules, *Methods Enzymol. 339*, 204−238.
25. Glynn, I. M., and Richards, D. E. (1982) Occlusion of rubidium ions by the sodium−potassium pump: its implications for the mechanism of potassium transport, *J. Physiol. 330*, 17−43.
26. Esmann, M., Fedosova, N. U., and Maunsbach, A. B. (2000) Protonation-dependent inactivation of Na, K-ATPase by hydrostatic pressure developed at high-speed centrifugation, *Biochim. Biophys. Acta 1468*, 320−328.
27. Rossi, R. C., and Nørby, J. G. (1993) Kinetics of K^+-stimulated dephosphorylation and simultaneous K^+ occlusion by Na,K-ATPase, studied with the K^+ congener Tl^+, *J. Biol. Chem. 268*, 12579−12590.
28. Glynn, I. M., Hara, Y., Richards, D. E., and Steinberg, M. (1987) Comparison of rates of cation release and of conformational change in dog kidney Na, K-ATPase, *J. Physiol. 383*, 477−485.
29. Redfield, A. G. (1965) The theory of relaxation processes, *Adv. Magn. Reson. 1*, 1−32.
30. Abragam, A. (1961) *Principles of Nuclear Magnetism*, Clarendon Press, Oxford, U.K.
31. Esmann, M., Horvath, L. I., and Marsh, D. (1987) Saturation transfer electron spin resonance studies on the mobility of spinlabeled Na, K-ATPase in membranes from *S. acanthias*, *Biochemistry 26*, 8675−8683.
32. Doyle, D. A., Cabral, J. M., Pfuetzner, R. A., Kuo, A., Gulbis, J. M., Cohen, S. L., Chait, B. T., and MacKinnon, R. (1998)

Structure of the potassium **c**hannel: Molecular basis of K^+ conduction and selectivity, *Science 280*, 69−77.
33. Sørensen, T. L. M., Clausen, J. D., Lund Jensen, A. M., Vilsen, B., Møller, J. V., Andersen, J. P., and Nissen, P. (2004) Localization of a K^+-binding site involved in dephosphorylation of the sarcoplasmic reticulum Ca^{2+}-ATPase, *J. Biol. Chem. 279*, 46355−46358.
34. Gouaux, E., and MacKinnon, R. (2005) Principles of selective ion transport in channels and pumps, *Science 310*, 1461−1465.
35. Hasenauer, J., Huang, W.-H., and Askari, A. (1993) Allosteric regulation of the access channels to the Rb^+ occlusion sites of (Na^+ + K^+)-ATPase, *J. Biol. Chem. 268*, 3289−3297.
36. Grisham, C. M., Gupta, R. K., Barnett, R. E., and Mildvan, A. S. (1974) Thallium-205 nuclear relaxation and kinetic studies of sodium and potassium ion-activated adenosine triphosphatase, *J. Biol. Chem. 249*, 6738−6744.
37. Zhou, Y., and MacKinnon, R. (2004) Ion binding affinity in the cavity of the KcsA potassium channel, *Biochemistry 43*, 4978−4982.
38. Cavanagh, J., Fairbrother, W. J., Palmer A. G., III, and Skelton, N. J. (1996) *Protein NMR Spectroscopy: Principles and Practice*, Academic Press, San Diego, CA.

BI060642K